



Structural Analysis of Powdered Manganese(II) of 1,10-Phenanthroline (phen) as Ligand and Trifluoroacetate (TFA) as Counter anion

KRISTIAN HANDOYO SUGIARTO¹, CAHYORINI KUSUMA WARDANI¹,
HARI SUTRISNO¹ and MUHAMMAD WAHYU ARIF WIBOWO¹

Department of Chemistry Education, Yogyakarta State University, Indonesia.

*Corresponding author: sugiyarto@uny.ac.id

<http://dx.doi.org/10.13005/ojc/340216>

(Received: December 21, 2017; Accepted: March 01, 2018)

ABSTRACT

The complex containing manganese(II), 1,10-phenanthroline (phen) as ligand and trifluoroacetate (TFA) as counter anion has been prepared and characterized. The electrical equivalent conductance, metal content, and TGA-DTA analysis suggests the complex to be $[\text{Mn}(\text{phen})_3](\text{TFA})_2 \cdot 1.35\text{H}_2\text{O}$. The magnetic moment was found to be normal high-spin paramagnetic for 5 unpaired electrons in the electron configuration of manganese(II). The electronic spectral bands indicates the five possible spin-forbidden transitions of sextet ground state to quartet excited states. The IR spectral data signify the mode of vibrations typical for phenanthroline as well as TFA, while the images of SEM-EDX photographs confirm the existence of the corresponding elemental content, they reflect high crystallinity of the complex as evidence of the sharp peaks of the corresponding powdered diffractogram. The analysis of powder XRD refined by Le Bail program was found to be structurally triclinic symmetry of *P*1 for the cationic complex with the cell parameters of $a = 13.6422\text{\AA}$; $b = 18.2792\text{\AA}$; $c = 23.8741\text{\AA}$; $\alpha = 114.4245^\circ$; $\beta = 94.8337^\circ$; $\gamma = 99.7977^\circ$; $V = 5261.6714\text{\AA}^3$, $Z = 1$; with *figure of merit*: $R_p = 1.31$; $R_{wp} = 2.39$; $R_{exp} = 0.56$; Bragg R-Factor = 0.04; and GOF = 18.00.

Keywords: Phenanthroline, Manganese(II), Trifluoroacetate, Rietica, Le Bail analysis.

INTRODUCTION

Synthesis and characterisation of complexes which were composed of transition metals, phenanthroline (phen) as ligand, and various counter ions, NO_3^- , BF_4^- , ClO_4^- , PF_6^- have

been reported long time ago¹⁻². However, the cell parameters of a single crystal of tris(phenanthroline) manganese(II) cation with any counter anion is, in fact, not easy to confirm, meaning that the preparation of single crystals seem unsuccessful. The chemistry of supramolecular tris(phenanthroline)



This is an Open Access article licensed under a Creative Commons Attribution-NonCommercial-ShareAlike 4.0 International License (<https://creativecommons.org/licenses/by-nc-sa/4.0/>), which permits unrestricted NonCommercial use, distribution and reproduction in any medium, provided the original work is properly cited.

manganese(II) cation has been reported to associate with I_3^- and I_5^- ions in the single crystals of $[Mn(phen)_3](I_3)_2$ ³ and $[Mn(phen)_3]I_8$ ⁴. Quite recently, the single crystal of simple perchlorate anion of $[Mn(phen)_3]^{2+}$ was isolated, but it was also known together with carbonic acid⁵.

Trifluoroacetic acid, H-TFA, is known a strong acid. The corresponding *pKa* is about 0.23 compared to a *pKa* of 4.76 for the acetic acid and thus being about 100,000 times stronger⁶. It is associated with the strongest electronegativity of fluorine atoms which leads to the electron-withdrawing character of the trifluoromethyl group. This results in weakening the oxygen-hydrogen bond and therefore stabilising the conjugate base of anion. Thus, it might be considered in the same group of strong acids with *pKa* less than one, such as hydroiodic, hydrobromic, hydrochloric, perchloric, chloric, nitric and (mono)sulfuric acids⁷.

For these reasons, the TFA would be possible to be a counter anionic role in cationic complex synthesis. However, the 3d cationic transition complex of TFA has not been much observed, and it seems the only cationic mercuracycle was reported⁸. In fact the monodentate coordinated TFA to gold (I)⁹ and to cobalt(II)¹⁰ in a polymer complexes were observed. Complex of diisopropylammonium trifluoroacetate has also been synthesized and found to be monodentate coordinated TFA with hydrogen bonding of N-H...O¹¹. With transition metals, Ru, Os, and Ir, hydrogen bonding of TFA were produced¹². With the monodentate ligand of pyridine (*py*), some molecular complexes of $M(Py)(CF_3CO_2)_2$ where $M=Co(II)$, $Ni(II)$, and $Cu(II)$, were isolated, indicating the coordinated TFA as a ligand rather than counter anion¹³.

The previous works clearly involved monodentate organic ligands, and it is readily understood that the TFA might prefer to coordinate as anionic ligand also. Thus, by involving relatively strong coordinated bidentate ligand such as 1,10-phenanthroline, the tendency of TFA to be mono/bi-dentate anionic ligand might be reduced and a cationic complex should result.

Thus the synthesis of manganese(II) complex of phenanthroline and TFA anion should be useful in understanding the ionic-molecular characteristic of the complex. The powder-XRD of the complex may be refined following Rietica method and this should lead to the structural lattice parameters, being comparable to some known single crystal structures as for example described by Polyanskaya *et al.*,¹⁴ and Wang¹⁵, and it is the main idea of this work. In the last two complexes the corresponding magnetic moment and electronic spectral data have not been reported yet.

EXPERIMENTAL

Materials

The main chemicals, nickel nitrate hexahydrate ($Ni(NO_3)_2 \cdot 6H_2O$), 1,10-phenanthroline ($C_{12}H_8N_2$), sodium trifluoroacetate (CF_3COONa), calcium nitrate ($Ca(NO_3)_2$), nickel sulfate ($NiSO_4$), calcium chloride ($CaCl_2$), ammonium nitrate (NH_4NO_3), aluminium nitrate ($Al(NO_3)_3 \cdot 6H_2O$), and iron(III) chloride ($FeCl_3$) were purchased from Sigma-Aldrich. All the reagents were used without further purification.

Preparation of Tris(phenanthroline)manganese(II) Trifluoroacetate

The mixture of about 5 mL solution of 0.32 mol phenanthroline in water with three drops of ethanol to clearly dissolve and about 10 mL of an aqueous solution of 0.1 mol $Mn(NO_3)_2$ was warmed while well stirring to obtain a homogeneous solution. A saturated aqueous solution of CF_3COONa (0.4 mol in 5 mL) which was stoichiometrically in excess was added to the mixture. It was then concentrated on heating, and the powdered complex which was precipitated on scratching while cooling was filtered, washed with a minimum of cold water, and then let the precipitate dry in exposure.

Physical Characterization

Magnetism. The magnetic moment of the complex was calculated through the measurement of the susceptibility for powdered samples which were obtained on magnetic susceptibility balance of Auto Sherwood Scientific 240V-AC model. This was calibrated with $CuSO_4 \cdot 5H_2O$. The corrected diamagnetism using Pascal's constant¹⁶ was applied to the molar magnetic susceptibility data

on the calculation of effective magnetic moment (μ_{eff}) following the formula, $\mu_{\text{eff}} = 2.828 \sqrt{X_M \cdot T}$ BM.

IR and UV-Vis Spectra. The IR spectrum of the sample which was set on the cell with potassium bromide pellets was recorded on a FTIR Spectrophotometer ABB MB3000 at 500 - 4000 cm^{-1} . UV-Vis spectrum of the powdered complex was recorded on a spectrophotometer of Pharmaspec UV 1700. The powders were spread on a thin glass adhered with ethanol. It was then put in the cell holder and the spectrum was recorded at 200-1000 nm. The spectrophotometer UV-V is Shimadzu 2400 PC Series was applied for recording the spectrum of complex in solution.

Ionic Property and Metal Content. The ionic character of the complex was based on the data of equivalent electrical conductance recorded using a conductometer Lutron CD-4301 calibrated with 1.0 M potassium chloride at 25 $^{\circ}$. The data obtained were compared to those of known ionic solutions, NH_4NO_3 , CaCl_2 , $\text{Ca}(\text{NO}_3)_2$, NiSO_4 , MnSO_4 , FeCl_3 , and $\text{Al}(\text{NO}_3)_3$, which were also recorded on the same instrument. The metal content of the complex was estimated as observed by Atomic Absorption Spectrophotometer model of PinAAcle 900T Perkin Elmer.

TGA-DTA (Thermogravimetric Analysis and Differential Thermal Analysis). Thermal decomposition of the complex, $[\text{Mn}(\text{phen})_3](\text{CF}_3\text{COO})_2 \cdot 1.35\text{H}_2\text{O}$, was performed up to 600 $^{\circ}\text{C}$ under nitrogen, to confirm the loss of particular materials contained in the compound. Thus, the loss of hydrated molecule of water and decomposition of other materials were performed on Diamond (Perkin Elmer Instruments), and simultaneous TGA-DTA graphs were obtained by a model NETZSCH STA

409C/CO thermal analyzer within the rate of 10 $^{\circ}\text{C}/$ minutes.

X-Ray Powder Diffraction. The X-ray diffractogram of the powdered complex was collected using a Rigaku Miniflex 600 40 kW 15 mA Benchtop Diffractometer, with $\text{CuK}\alpha$: $\lambda = 1.5406 \text{ \AA}$. The powdered complex was spread on the glass plate which was then set on the cell holder. The data of reflection were collected in a scan mode with interval of 0.04 steps per 4 seconds within 2 h at 2-90 degree of 2θ . The X-Ray diffractogram then was refined according to Rietica program of Le Bail method at the range 5-60 degree of 2θ which was run within 75 cycles.

SEM-EDX (Scanning Electron Microscopy with Energy Dispersive X-Ray). The SEM images of the complex were recorded in JEOL JED-2300 model to confirm the crystallinity as well as the content of the main elements.

RESULTS AND DISCUSSION

Conductance, AAS, TGA-DTA and Chemical Formula

Direct interactions of manganese(II) nitrate and the phenanthroline in solution resulted in a light yellow-greenish solution of cationic complex which precipitated on the addition of excessive TFA salt. The equivalent electrical conductance of this complex was estimated on the basis of known simple compounds, and the results of measurement are listed in Table 1. It was found that the conductance value for the complex is in the range of those for ionic compounds of three ions per molecule, and hence the empirical formula of $[\text{Mn}(\text{phen})_n](\text{CF}_3\text{COO})_2 \cdot x\text{H}_2\text{O}$ is then proposed for this complex, indicating a typical uncoordinated anion of TFA.

Table 1: Equivalent electric conductance of the complex and some known salts in aqueous solutions

Compounds	Equivalent conductance ($\Delta\text{c})\Omega^{-1}\text{cm}^2 \text{mol}^{-1}$	Amount ratio of cation/anion	Number of ions per molecule
NH_4NO_3	160.429	1 : 1	2
NiSO_4	118.355	1 : 1	2
MnSO_4	119.612	1 : 1	2
$\text{Ca}(\text{NO}_3)_2$	379.355	1 : 2	3
$\text{Al}(\text{NO}_3)_3$	519.095	1 : 3	4
FeCl_3	476.975	1 : 3	4
$[\text{Mn}(\text{phen})_n](\text{CF}_3\text{COO})_2 \cdot x\text{H}_2\text{O}$	209.125	1 : 2	3

The metal content observed in the atomic absorption spectral data (6.9% in mass) followed by TGA data should estimate the coordination number (n) and the number of hydrates (x) of the empirical formula. As shown in Fig. 1, the mass loss of 2.856% in the first stage at 80-90 °C is believed due to the loss of $1.35\text{H}_2\text{O}$ (ca. 2.873%). While the loss of mass in the second-third-fourth stages are complicated to identify, the residual mass of 18.624% at 300-500 °C seems to be due to $\alpha\text{-Mn}_2\text{O}_3$ (ca. 18.664%)¹⁷, leading to Mn content of 6.96% (ca. 6.50%). Theoretically, the mass loss of

TFA and phen are 25.444 and 60.857 %, respectively, while total loss in the second-fourth stages (150-400 °C) is only about 78.52 %. The only thing we can say is that during the loss of TFA, the oxygen atom might react with metal to form final product of Mn_2O_3 .

Thus in summary, the percentage of each entity in the powdered complex as shown in Table 2 might confirm the formula proposed, $[\text{Mn}(\text{phen})_3](\text{CF}_3\text{COO})_2 \cdot 1.35\text{H}_2\text{O}$, as expected also from stoichiometric preparation.

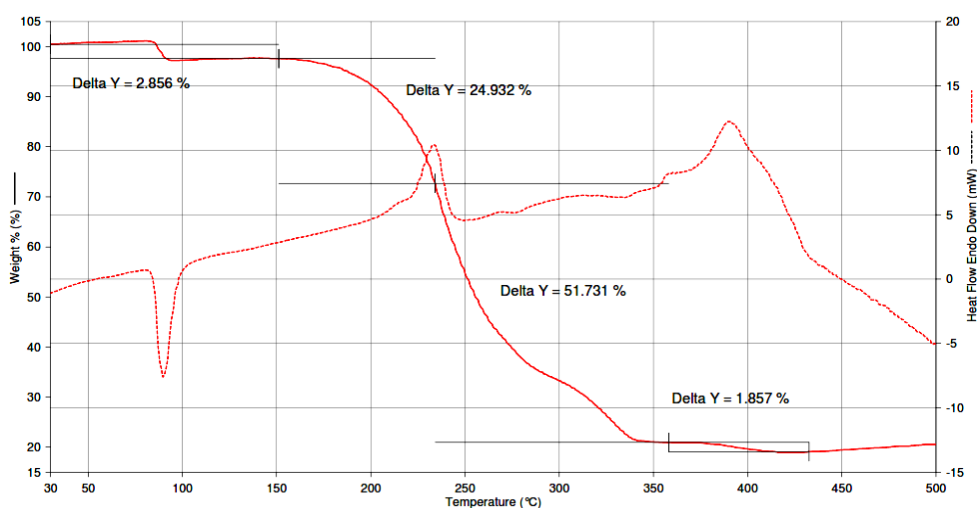


Fig. 1. The TGA-DTA of $[\text{Mn}(\text{phen})_3](\text{CF}_3\text{COO})_2 \cdot 1.35\text{H}_2\text{O}$ at 30-500 °C

Table 2: Entity Found in $[\text{Mn}(\text{phen})_3](\text{CF}_3\text{COO})_2 \cdot 1.35\text{H}_2\text{O}$

Type	Mn	$1.35\text{H}_2\text{O}$	$2(\text{CF}_3\text{COO})$	$3(\text{phen})$	Residue Mn_2O_3
Calculated	6.5	2.873	25.444	60.857	18.664
Found	6.9	2.856	24.932	51.731+1.857	18.624
Method	AAS	TGA	TGA	TGA	TGA

Magnetic Moment

The effective magnetic moments of the complex calculated from molar magnetic susceptibility data which were collected on measurement for the three separated preparation were found to be 5.81, 5.89, and 5.92 BM at 291K, being normal paramagnet. These reflect to the spin-only value (μ_s) which corresponds to five unpaired electrons in the electron configuration of Mn(II). It is normal values in an octahedral environment as observed by some literatures to be

5.89-6.16 BM for various different ligands¹⁸⁻²¹. Much lower in magnetism, however, have been reported to the molecular complex of $[\text{Mn}(\text{Val})_2(\text{phen})]^{22}$, the magnetic moment being only 5.12 BM.

Electronic Spectrum

The UV-Vis. spectrum of the powder complex as depicted in Fig. 2, demonstrates clearly three absorption bands (ν_3 , ν_4 , and ν_5) at high range of energy, 28000-40000 cm^{-1} . Another lower shoulder at 24000-26000 cm^{-1} (ν_2) and another

bump at 17000 cm^{-1} (ν_1) might establish the possible electronic transitions following Tanabe-Sugano diagram for MnF_2 and comparably observed by other literatures^{18-19, 23}.

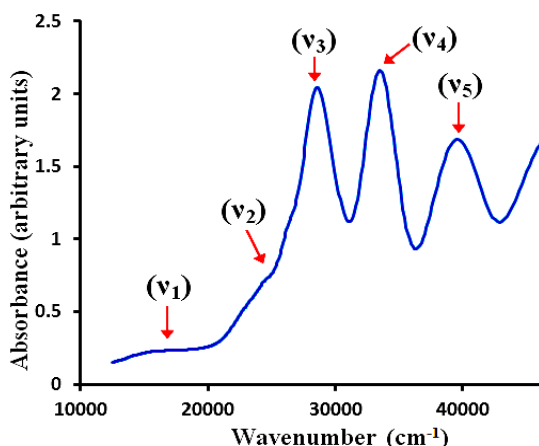


Fig. 2. UV-Vis spectrum of $[\text{Mn}(\text{phen})_3](\text{CF}_3\text{COO})_2 \cdot 1.35\text{H}_2\text{O}$

Thus the fully high-spin state of the complex as indicated by the magnetic moment values leads to the ground state of ${}^6A_{1g}$, and since other sextet excited states are not possible there should be no spin-allowed transitions, and thus the spin-forbidden transitions to quartet states govern the electronic absorption bands. Therefore, transitions of ${}^6A_{1g} \rightarrow {}^4T_{1g}({}^4G)$, ${}^6A_{1g} \rightarrow {}^4T_{2g}({}^4G)$, ${}^6A_{1g} \rightarrow {}^4E_g, {}^4A_{1g}({}^4G)$, ${}^6A_{1g} \rightarrow {}^4T_{2g}({}^4D)$, and ${}^6A_{1g} \rightarrow {}^4E_g({}^4D)$ are then proposed to occur at 17000 cm^{-1} (ν_1), $24000\text{--}25000\text{ cm}^{-1}$ (ν_2), 28000 cm^{-1} (ν_3), 35500 cm^{-1} (ν_4), and at 39500 cm^{-1} (ν_5), respectively.

Infrared Spectrum

IR spectrum of this complex was collected at the range of $500\text{--}4000\text{ cm}^{-1}$ (Fig. 3). By overlaying the corresponding spectrum of TFA anion, the main purpose to assign the typical vibration bands of phenanthroline (red) might come straight forward. The broad band at about 3418 and 3433 cm^{-1} might be due to $-\text{OH}$ stretching of H_2O molecules as indicated by the formula proposed, and also observed by Shad *et al.*,²⁴ at about 3441 cm^{-1} , though Kumar *et al.*,²⁵ assigned C-C aromatic at 3430 cm^{-1} . Another band at 3059 and $2341\text{--}2361\text{ cm}^{-1}$ should be due to stretching vibration of C-H bonds of phenanthroline which were reported by Chen *et al.*,²⁶ at 3064 cm^{-1} , and Tosonian *et al.*,²⁷ at $3051\text{--}3068\text{ cm}^{-1}$.

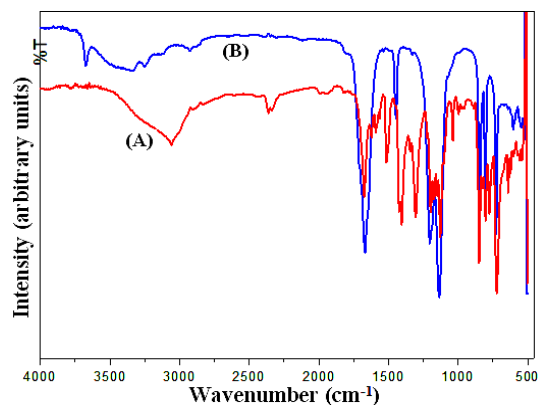


Fig. 3. IR spectrum of $[\text{Mn}(\text{phen})_3](\text{CF}_3\text{COO})_2 \cdot 1.35\text{H}_2\text{O}$ (A) and of TFA (B)

The typical ring modes of phenanthroline ($\nu_{\text{C-C}}$ and $\nu_{\text{C-N}}$) in the range of $1700\text{--}600\text{ cm}^{-1}$, might be strongly observed at 1620 , 1589 , 1415 , 1304 , and 775 cm^{-1} , being comparably observed by Ramalakshmi *et al.*, for the corresponding iodide³. Other stretching modes are due to TFA (blue), $\nu_{\text{C-F}}$, $\nu_{\text{C-O}}$ and $\nu_{\text{C-O}}$, being observed at 1670 , 1443 , 1203 , 1134 , 845 , 802 , 725 , and 602 cm^{-1} .

X-Ray Powder Diffraction and Structural Refinement

Diffractiongram of the powdered $[\text{Mn}(\text{phen})_3](\text{CF}_3\text{COO})_2 \cdot 1.35\text{H}_2\text{O}$ was recorded and then analysed. As shown in Fig. 4, the black signs (+) are the experimental data, the red full line represents the result of refinement due to Rietica-Le Bail program performed at the range of $5\text{--}60$ degree of 2θ within 75 cycles, the blue bar-lines are the expected lines of the symmetry and space group model, while the green line reflects the intensity difference between the experimental data (black) and the result of refinement (red). Clearly, the red full line does pass through almost all of the black experimental signs, as also demonstrated by almost flat green line. This suggests that the refinement of the model fitting to the experimental data is almost perfect. The detailed cell parameters of the structure are recorded in Table 3 together with similar data for some known single crystals of the same cations. Therefore, this complex synthesized in this work might be considered as triclinic symmetry of $P1$.

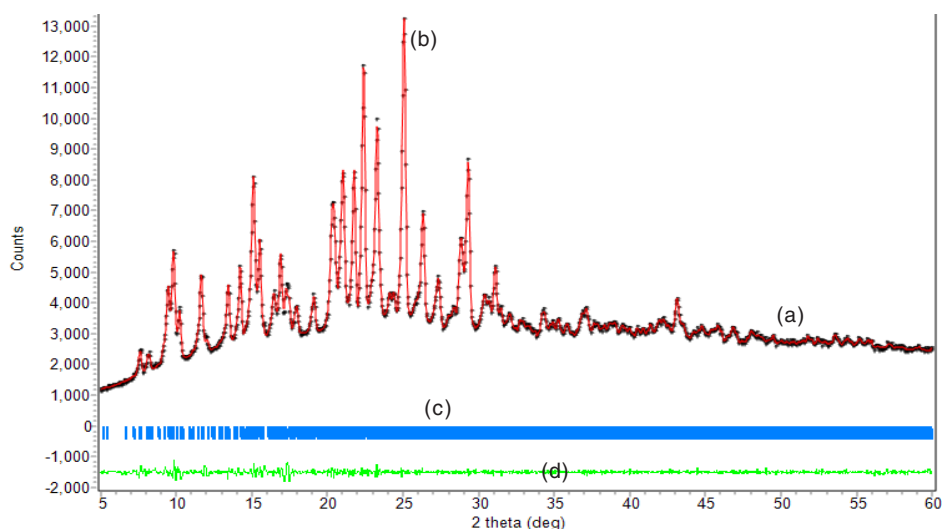


Fig. 4. XRD profile of $[\text{Mn}(\text{phen})_3](\text{CF}_3\text{COO})_2 \cdot 1.35\text{H}_2\text{O}$ (a-black), the refinement on triclinic symmetry of *PI* (b-red) with its position of 2θ (c-blue), and the intensity difference between the black and the red lines (d-green)

Table 4: Detailed cell parameters of $[\text{Mn}(\text{phen})_3] \text{X}$, where $\text{X} = (\text{TFA})_2 \cdot 1.35\text{H}_2\text{O}$ (a)*, $(\text{CF}_3\text{SO}_3)_2 \cdot 6.5\text{H}_2\text{O}$ (b)*²⁸, $(\text{B}_6\text{H}_7)_2$ (c)¹⁴, Cl_2 (d)¹⁵, $(\text{I}_3)_2$ (e)³, $(\text{ClO}_4)_2(\text{H}_2\text{CO}_3)_2$ (f)⁵, and $(\text{Rdtp})_2$ (g)²⁹. (*this work due to Le Bail method of Rietica program)

X	(a)*	(b)* ²⁸	(c) ¹⁴	(d) ¹⁵	(e) ³	(f) ⁵	(g) ²⁹
Symmetry	Triclinic	Triclinic	Triclinic	Tetragonal	Hexagonal	Triclinic	Monoclinic
Space Group	PI	PI	PI	I41/a (no. 88)	R3 (no. 148)	PI	C2
α (Å)	13.6422	12.6338	10.3131	35.922(1)	16.456(3)	12.6685(10)	16.55(1)
b (Å)	18.2792	17.0627	13.4839	11.8977(8)	16.456(3)	12.9049(2)	17.50(1)
c (Å)	23.8741	22.4810	15.1132		25.864(4)	13.2145(10)	17.46(1)
α (°)	114.4245	106.8768	97.696			86.341(10)	
β (°)	94.8337	110.9014	108.324			74.337(10)	93.0(1)
γ (°)	99.7977	99.56265	102.211			73.701(10)	
V (Å ³)	5261.6714	4130.4170	1903.92	15352.4(12)	6066(2)	1996.39(4)	4680.0
Z	1	1	2	16	6	4	4
Figure of merit:							
R_p	1.31	3.67					
R_{wp}	2.39	7.34					
R_{exp}	0.56	3.61					
Bragg R-Factor	0.04	0.09					
GOF	18.00	4.133	n.a.	n.a.	n.a.	n.a.	n.a.

SEM-EDX

The SEM photographs of $[\text{Mn}(\text{phen})_3](\text{TFA})_2 \cdot 1.35\text{H}_2\text{O}$ on various magnification reflects the high crystallinity of the complex which is

also clearly demonstrated by the corresponding diffractogram which shows sharp peaks. Fig. 5(d) might indicate triclinic crystal system as resolved by the Rietica program on the diffractogram.

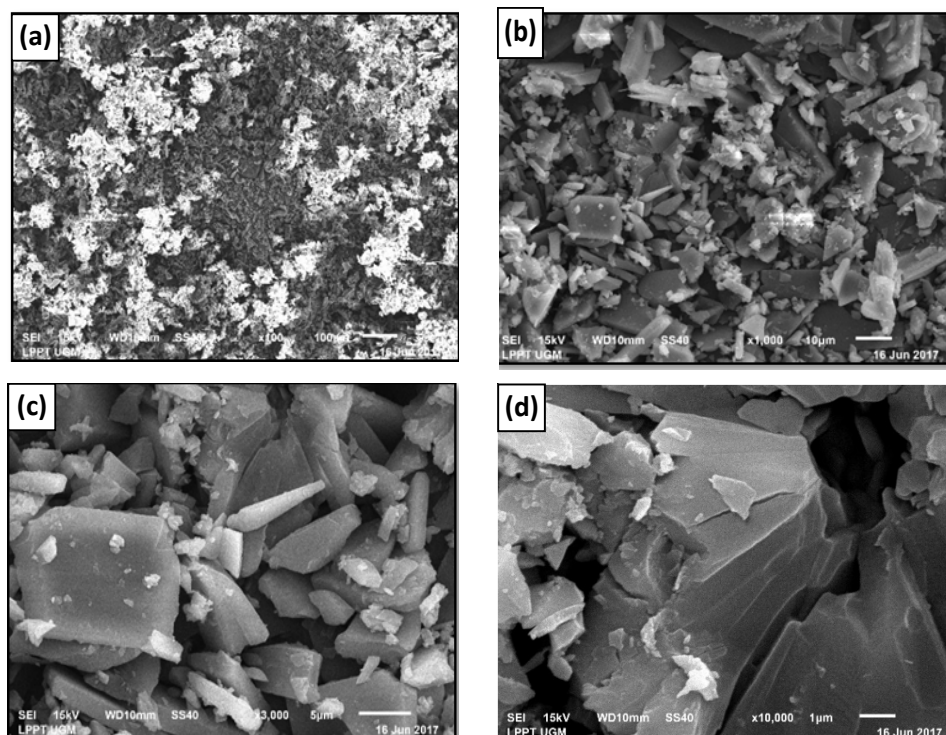


Fig. 5. SEM photographs of $[\text{Mn}(\text{phen})_3](\text{CF}_3\text{COO})_2 \cdot 1.35\text{H}_2\text{O}$ at magnification of 100x (a), 1000x (b), 3000x (c) and 10,000x (d)

The corresponding energy dispersive X-ray (EDX) analysis resulted from the selected surface as shown in Fig. 6(a) strongly demonstrates the existence of all elements (Fig. 6(b)) except the hydrogen atom, and therefore, the percentage ratio

of the number of atoms, being Mn: 1(2%), C:25.7(51.43%), N:12.7(25.56%), O: 6.6(13.34%), and F: 3.8(7.67%) clearly does not reflect the accurate quantitative stoichiometry.

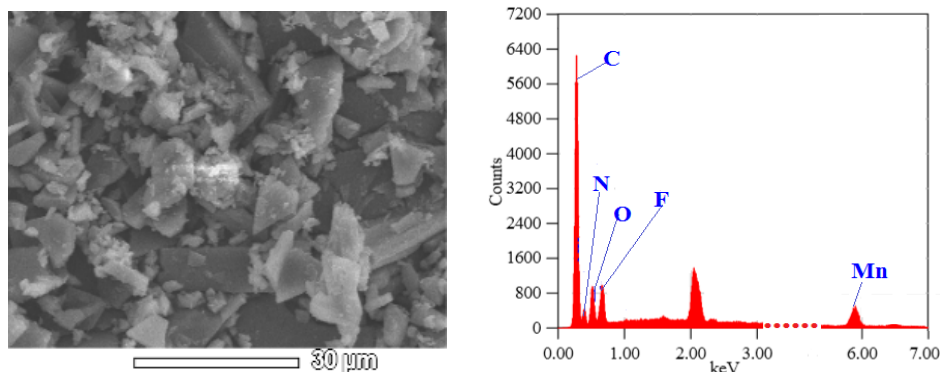


Fig. 6. The image of selected surface of $[\text{Mn}(\text{phen})_3](\text{CF}_3\text{COO})_2 \cdot 1.35\text{H}_2\text{O}$ and its EDX analysis result showing the content of elements

CONCLUSION

The complex of $[\text{Mn}(\text{phen})_3](\text{CF}_3\text{COO})_2 \cdot 1.35\text{H}_2\text{O}$ has been successfully prepared and found to be normal paramagnet of high spin Mn(II). The

electronic spectral property of the powdered complex might be resolved into five bands associated with the spin-forbidden transitions of the sextet ground state (${}^6A_{1g}$) to quartet states of ${}^4T_{1g}({}^4G)$, ${}^4T_{2g}({}^4G)$, 4E_g , ${}^4A_{1g}({}^4G)$, ${}^4T_{2g}({}^4D)$, and ${}^4E_g({}^4D)$.

The IR spectral properties signify the mode of vibrations characteristic for phenanthroline and TFA groups. The SEM images show high crystallinity of the powder which is also reflected by its sharp peaks of the diffractogram. Following Rietica method of Le Bail program the diffractogram was analysed to have triclinic symmetry of *PI* space group.

ACKNOWLEDGMENT

Authors thank to the Faculty of Mathematics and Natural Science (Yogyakarta State University) because for the funding, DIPPA-2017 for this work.

REFERENCES

- Ito T.; Tanaka N.; Hanazaki I.; Nagakura S. *Bulletin of the Chemical Society of Japan.*, **1969**, *42*, 702-709.
- Lee C. S.; Gorton E. M.; Neumann H. M.; Hunt Jr. H. R. *Inorg. Chem.* **1966**, *5*, 1397-1399.
- Ramalakshmi D.; Reddy K. R.; Padmavathy D.; Rajasekharan M. V.; Arulsamy N.; Hodgson D. J. *Inorganica Chimica Acta.*, **1999**, *284*, 158-166.
- Horn C.; Scudder M.; Dance I. *Cryst. Eng. Comm.*, **2001**, *1*, 1-8.
- Kani I.; Atlier Ö.; Güven K. *J. Chem. Sci.*, **2016**, *128*, 523-536.
- Trifluoroacetic Acid. Available at: http://www.commonorganicchemistry.com/Common_Reagents/Trifluoroacetic_Acid/Trifluoroacetic_Acid.htm.
- Table of Acids with Ka and pKa Values (Compiled from Appendix 5 Chem 1A, B, C Lab Manual and Zumdahl 6th Ed. The pKa values for organic acids can be found in Appendix II of Bruice 5th Ed.). Available at: <http://clas.sa.ucsb.edu/staff/Resource%20folder/Chem109ABC/Acid,%20Base%20Strength/Table%20of%20Acids%20and%20pKas.pdf>.
- Zheng Z.; Knobler C. B.; Curtis C. E.; Hawthorne M. F. *Inorg. Chem.*, **1995**, *34*, 432-435.
- Tunyogi T.; Deák A. *Acta Cryst.* **2010**, *C66*, m133-m136.
- Peedikakkal A. M. P.; Song Y. M.; Xiong R. G.; Gao S.; Vittal J. J. *Eur. J. Inorg. Chem.*, **2010**, 3856-3865.
- Reiß G. J.; Meyer M. K. *Z. Naturforsch.*, **2010**, *65b*, 479-484.
- Robinson S. D.; Sahajpal A. *J. Chem. Soc. Dalton Trans.*, **1997**, 3349-3351.
- Agambar C. A.; Orrell K. G. *J. Chem. Soc., (A)*, **1969**, 897-904.
- Polyanskaya T. M.; Drozdova M. K.; Volkov V. V.; Myakishev K. G. *Journal of Structural Chemistry.*, **2009**, *50*, 368-372.
- Wang X., *Z. Kristallogr.*, **2013**, *NCS 228*, 5-6.
- Figgis B. N. and Lewis, J., *Modern Coordination Chemistry*, Edited by Lewis, J., and Wilkins, R. G., Interscience: New York, **1960**: 400.
- Pattanayak J.; Rao V. S.; Maiti H. S.; *Thermochimica Acta.*, **1989**, *153*, 193-204.
- Singh B. K.; Mishra P.; Prakash A.; Narendar Bhojak N. *Arabian Journal of Chemistry.*, **2012 (2017)**, *10*, S472-S483 (to be published). <https://doi.org/10.1016/j.arabjc.2012.10.007>
- Verma R.; *International Journal of Pharmaceutical Sciences and Research.*, **2017**, *8*(3), 1504-1513.
- Devereux M.; McCann M.; Leon V.; Kelly R.; O'Shea D.; McKee V. *Polyhedron.*, **2003**, *7*, 3187-3194.
- Devereux M.; McCann M.; Leon V.; Geraghty M.; McKee V.; Wikaira J. *Metal Based Drugs.* **2001**, *7*, 275-288.
- Fayad N. K.; Al-Noor T. H.; Mahmood A. A.; Malih I. K. *Chemistry and Materials Research.*, **2013**, *3*, 66-73.
- Lever A. B. P., *Inorganic Electronic Spectroscopy*, Second Edition, Elsevier: New York, **1968**: p. 293.
- Shad H. A.; Thebo K. H.; Ibpoto Z. H.; Malik M. A.; O'Brien P.; Raftery J. *Journal of Coordination Chemistry.*, **2011**, *64*, 2353-2360.
- Kumar S. P.; Suresh R.; Giribabu K.; Manigandan R.; Munusamy S.; Muthamizh S.; Narayanan V. *International Journal of ChemTech Research.*, **2014**, *6*, 3280-3283.
- Chen H.; Xu X.-Y.; Gao J.; Yang X. J.; Lu L. D.; Wang X. *Acta Phys. -Chim. Sin.*, **2006**, *22*, 856-859.
- Tosoniani S.; Ruiz C. J.; Rios A.; Frias E.; Eichler J. F., *Open Journal of Inorganic Chemistry.* **2013**, *3*, 7-13.
- Sugiyarto K. H.; Saputra H. W.; Permanasari L.; Kusumawardani C. *AIP Conference Proceedings.*, **2017**, *1847*, (040006)1- 7.
- Drew M. G. B.; Hasan M.-I.; Hellot Y. *Polyhedron.*, **1989**, *8*, 1853-1854.